HHS Public Access

Author manuscript

J Biomed Mater Res A. Author manuscript; available in PMC 2018 April 12.

Published in final edited form as:

J Biomed Mater Res A. 2016 July ; 104(7): 1581–1590. doi:10.1002/jbm.a.35769.

Evaluation of the tissue response to alginate encapsulated islets in an omentum pouch model

Veronica Ibarra[1], **Alyssa A. Appel**[1], **Mark A. Anastasio**[2], **Emmanuel C. Opara**[3], and **Eric M. Brey**[1,4]

[1]Department of Biomedical Engineering, Illinois Institute of Technology, Chicago, Illinois

[2]Department of Biomedical Engineering, Washington University in St. Louis, St. Louis, Missouri

[3]Wake Forest Institute for Regenerative Medicine, Winston-Salem, Illinois

[4]Research Services, Edward Hines Jr. VA Hospital, Ines, IL

Abstract

Islet transplantation is currently in clinical use as a treatment for type I diabetes, but donor shortages and long-term immunosuppression limit broad application. Alginate microcapsules coated with poly-L-ornithine can be used to encapsulate islets in an environment that allows diffusion of glucose, insulin, nutrients, and waste products while inhibiting cells and antibodies. While clinical trials are ongoing using islets encapsulated in alginate microbeads, there are concerns in regards to long-term stability. Evaluation of the local tissue response following implantation provides insight into the underlying mechanisms contributing to biomaterial failure, which can be used to the design of new material strategies. Macrophages play an important role in driving the response. In this study, the stability of alginate microbeads coated with PLO containing islets transplanted in the omentum pouch model was investigated. Biomaterial structure and the inflammatory response were characterized by X-ray phase contrast (XPC) μCT imaging, histology, and immunostaining. XPC allowed evaluation of microbead 3D structure and identification of failed and stable microbeads. A robust inflammatory response characterized by high cell density and the presence of pro-inflammatory macrophages was found around the failed grafts. The results obtained provide insight into the local tissue response and possible failure mechanisms for alginate microbeads.

Keywords

X-ray phase contrast; alginate; biomaterial stability; inflammatory response; macrophages

INTRODUCTION

According to the American Diabetes Association, type I diabetes affects over 1.25 million Americans. While there is no cure for the disease, current treatment options include regular insulin injections or, in some cases, whole pancreas transplantation. Insulin injections only

Correspondence to: E. M. Brey; brey@iit.edu.

delay the progression of secondary complications such as retinopathy, nephropathy, and neuropathy resulting in lowering quality and expectancy of life.[1] Pancreas transplantation achieves normoglycemia by reestablishing insulin release.[2,3] However, the dependence on immunosuppression and limited availability of pancreata indicate the need for other treatment options.

Islet transplantation is an option in clinical use for some type 1 diabetic patients. However, the treatment is available to only a small subset of patients due to limited islet availability and the requirement of immunosuppressant therapies. These issues can be addressed, in part, by encapsulation of islets in a permselective biomaterial. Appropriately designed materials would allow transport of small molecules, while inhibiting antibodies and cells involved in rejection. Alginate-based materials have been amongst the most popular materials investigated and have reached clinical trials using both allogeneic and xenogeneic islet sources.[4]

Alginate is extracted from algae and has been used clinically for cell encapsulation, drug delivery, and tissue engineering applications. Alginate contains blocks of (1–4)-linked β-D-mannuronic acid and (M) and α-L-guluronic acid (G).[5,6] Alginate materials can be prepared by combining alginate with cross-linking agents, the most common being divalent cations such as Ca^{2+}, Ba^{2+}, Sr^{2+}. Poly-L-Lysine (PLL) and Poly-L-ornithine (PLO) are the most common materials used as coatings for alginate materials. A PLO coating can increase mechanical strength and restrict higher molecular weight components which in combination with alginate, creates a semipermeable structure that protects cells from the immune system while allowing exchange of oxygen, nutrients, waste, and insulin.[7,8] Alginate materials coated with permselective membranes have demonstrated successful protection of xeno-transplantation of islets, opening the possibility to obtain more tissue sources which may help to overcome human donor shortages. [9–11]

Alginate microbeads can provide a protective barrier for cells, but this is dependent on the stability of the biomaterial system and the local tissue response. There appear to be significant concerns in regards to long-term stability of the beads since the underlying mechanisms that lead to biomaterial failure are not established. Graft biocompatibility, transplantation site and stability of the biomaterial system may all contribute to the overall stability.[4] These factors can be interdependent with biomaterial properties driving the local inflammatory response and potential failure of the system. Evaluating the local tissue response to biomaterials can help identify potential mechanisms that lead to failure. This information can inform the design of future materials with improved biological outcomes.

Macrophages play an important role in determining the ultimate outcome of an implanted biomaterial. Macrophage phenotype around a biomaterial can predict the long-term response, either remodeling/healing or prolonged inflammation.[12] Macrophages can take on a broad range of phenotypes driven by the material properties and biology of the transplant site. At the first order level they can be categorized as either M1 or M2. The M1 phenotype is considered the pro-inflammatory macrophage phenotype and is often associated with a poor long-term biomaterial response. The M2 phenotype is associated with tissue repair, a constructive remodeling response and is considered an anti-inflammatory phenotype.[13–15]

The stability of alginate materials and host response may be inferred, in part, by analyzing the macrophage phenotype in the tissue surrounding the implanted material.

In this study, the stability of alginate microbeads with and without islets implanted in an omentum pouch was characterized by histological stains combined with X-ray phase contrast (XPC) imaging. The local macrophage phenotype around different bead structures was further evaluated to gain insight into potential failure mechanism. These results provide insight into the local tissue response to alginate microbeads implanted in an omentum pouch and possible failure mechanisms.

MATERIALS AND METHODS

Fabrication of alginate microbeads encapsulating islets

Low-viscosity-high-mannuronic-acid (LVM) and low-viscosity-high-guluronic-acid (LVG) alginate were purchased from Nova-Matrix (Sandvika, Norway). A solution of 0.1% poly-L-ornithine (PLO) was purchased from Sigma-Aldrich (St. Louis, MO). The crosslinking solution was prepared of 100 m*M* of $CaCl_2$ (Acros, NJ) and 0.9% of NaCl was used as the washing solution. Solutions were prepared in deionized water, pH balanced to 7.4 and stored at 4°C. Islets were isolated from Male Wistar rats (Harlan, Dublin, VA). Animal protocols were approved by the Wake Forest University Institutional Animal Care and Use Committee. Islets were isolated by collagenase digestion of pancreatic tissue.[16,17]

Islets were encapsulated using a technique previously described.[18–20] Briefly, 2000 islets/mL were dispersed in 1.5% LVM and the suspension was pumped at a constant flow rate of 1.4 mL/min through a high-throughput flow focusing microfluidic device. The microbeads where allowed to crosslink in 100 m*M* $CaCl_2$ for 15 min, washed and then incubated in 0.1% PLO for 20 min. After the microcapsules were coated with PLO, a final outer layer of 1.25% LVG was applied. The outer layer was crosslinked with 22 m*M* solution of $CaCl_2$ for 5 min and then washed with normal saline solution. The capsules were cultured overnight in RPMI 1640 medium and transplanted the next day.

The volume fraction of the alginate microbeads (φ) and the average radius of the openings between polymer chains ($\bar{r}$) were determined as described previously.[6] Briefly, empty microbeads were weighed following preparation and then dried for at least 48 h in an incubator at 37°C. The dry weight was determined and the volume fraction was calculated using Eq. (1). The average radius of the openings between polymer chains was calculated using Eq. (2).

$$\varphi = \frac{\frac{m_{dry}}{\rho_{alginate}}}{\frac{m_{dry}}{\rho_{alginate}} + \frac{m_{wet} - m_{dry}}{\rho_{water}}} \quad (1)$$

$$\bar{r} = \frac{k_s \varphi^{-1/2}}{2} \quad (2)$$

Animal model

Diabetes was induced in Male Lewis Rats (Harlan, Dublin, VA) via intraperitoneal injection of streptozotocin (STZ). Rats were defined as diabetic when blood glucose levels were higher than 400 mg/dL for 2 consecutive days. When diabetes was diagnosed, insulin pellets were inserted in the back of the neck to maintain animals' healthy levels before transplant studies. Alginate microspheres (800–1000 per animal) were transplanted in the omental tissue and a pouch was created by sewing with a Vicryl suture. In additional studies, alginate microbeads prepared under the same conditions but without islets were implanted in the same rat omentum pouch model.

XPC μCT

The entire omentum was harvested, including all beads and surrounding tissue. The samples were fixed in formalin and then the entire tissue imaged using an analyzer based XPC imaging system at the National Synchrotron Light Source at Brookhaven National Laboratory (Beamline X15A).[21] A monochromated 20 keV beam was utilized for X-ray imaging. The detector employed was an X-ray Imager VHR 1:1, CCD (Photonic Science Limited, UK) sensor (400 × 4008 pixels) with a detector pixel size of 9 μm. Using a [333] analyzer crystal reflection, the measurement data were acquired at 11 angular positions of the analyzer crystal ranging from −4 to +4 μrad to generate a rocking curve for each pixel in the detector for each tomographic view angle.[22–24] Five hundred tomographic intensity measurements were acquired over a 180° angular range for each analyzer-crystal orientation. At each tomographic view angle, three parametric MIR images that represent projected absorption, refraction and Ultra-small-angle-X-ray-scatter (USAXS) properties of the sample were computed.[25] From knowledge of the three MIR images computed at each tomographic view angle, a filtered back projection reconstruction method was employed to reconstruct volumetric images of the three MIR properties. MicroCT was performed to identify different soft tissues and alginate microbeads. Microbead structure was examined in 3D with XPC μCT.

Immunohistochemical staining

After XPC imaging, the tissues were processed for histology using standard methods and tissues were paraffin embedded. Samples were sectioned at 5 μm thickness and stained with hematoxylin and eosin and Masson's Trichrome. Serial sections of the omentum were also stained immunohistochemically to determine the presence of CD68 (pan-macrophage marker), CD163 (pro-healing marker), or CCR7 (pro-inflammatory marker) positive cells. Slides were deparaffinized and rehydrated in graded alcohols. Antigen Retrieval (Dako, CA) was used at a 1:10 dilution. The solution was brought to a boil and the slides incubated for 30 min. The solution was cooled and the slides were placed in acetone solution for 5 min. The slides were washed three times in PBS and then incubated in 3% H_2O_2 for 12 min to

block endogenous peroxidase. After rinsing with PBS the specimens were incubated in normal 1.5% horse serum (CD68, CD163) and 5% goat serum (CCR7) for 20 min. Overnight incubation was performed with the primary antibody CD68 (Clone ED1, Serotec, NC; dilution 1:50), CD163 (Clone ED2, Serotec, NC; dilution 1:25), or CCR7 (Abcam; 1:50,000). After overnight incubation, the sections were washed in PBS. The secondary antibody was added Biotinylated anti-mouse IgG (Vector, BA-2001, for CD68 and CD163) and Bio-tinylated anti-rabbit IgG (Vector, BA-1000, for CCR7) at a dilution of 1:200 for all antibodies. The antibodies were diluted in the corresponding blocking serum solution and incubated for 30 min (CD68) or 1 h (CD163, CCR7). The sections were washed in PBS and incubated with the Vectastain ABC reagent (VECTASTAIN ABC kit Peroxidase Mouse IgG, Vector, PK4002,) or VECTASTAIN Elite ABC Kit Rabbit IgG (Vector, PK6101). Incubation time for the ABC reagent was 30 min. After incubation, the slides were washed with PBS and distilled water. 3,3′-Diaminobenzidine (DAB, Invitrogen) was used to detect peroxidase activity at room temperature. Slides were washed with PBS and distilled water and counterstained with Gills Hematoxylin (Sigma-Aldrich). A PBS wash was performed and distilled water was added. Slides were mounted and cover slipped.

Histological and immunohistochemical analysis

An inverted microscope with an AxioCam MRc5 color camera (Carl Zeiss MicroImaging) was used to perform quantitative histomorphometric analysis to analyze a variety of tissue properties. Images were analyzed using Axiovision, an image analysis software (Carl Zeiss MicroImaging, Thornwood, NY). Failure rates of the alginate microbeads was obtained by defining a microbead as either stable or failed. Failure was based on identification of tissue or cellular infiltration observed in either the histological or XPC images. A stable bead was any microbead that was still intact and did not present any evidence of tissue invasion or breakage. For each sample, all alginate microbeads within a tissue section were analyzed and compared with XPC images. The number of beads in a given section ranged from 5 to 101.

The thickness of the tissue surrounding the alginate microbeads was identified in H&E images. Eight measurements of thickness were taken and averaged for each alginate microbead. The number of cells present around the tissue surrounding the alginate microbeads was quantified from the H&E stains. Number of cells over total tissue surrounding the microbeads indicated the cell density values. Microbeads from multiple sections of the omenta were analyzed (eight slides). Tissue thickness and cell density values of the tissue surrounding the microbeads was obtained for a maximum of 25 microbeads.

Immunostained slides were imaged using brightfield microscopy (Carl Zeiss MicroImaging). All image analysis was conducted using MATLAB software (Mathworks). Quantitative analysis was performed by measuring the total area of $CD68^+$, $CD163^+$, or $CCR7^+$ positive tissue and then dividing it by the total tissue area around the microbeads. The percentage of positive stain was obtained for failed alginate microbeads and stable alginate microbeads with and without islets. Sections from slides of $CD68^+$, $CD163^+$, or $CCR7^+$ stain were analyzed. A total of 8 slides were analyzed. For the three macrophage markers, the area of positive stain for a range of 14–21 microbeads was quantified.

Statistical methods

Statistical analysis was performed using SigmaStat. Statistical significance was determined using Student's *t* test, with a *p* values of less than 0.05 considered significant.

RESULTS

Islets were encapsulated in alginate microbeads coated with a permselective PLO layer and an outer alginate layer.[18] The conditions used were determined based on extensive studies for the optimal alginate composition and concentration for control of islet viability.[18,26] Under these conditions, the outer PLO results in a permselective membrane, preventing the passage of molecules >120 kDa in size into the inner alginate.[18] The inner core of alginate had a volume fraction of 0.016 ± 0.019 and average radius of the openings between polymer chains of approximately 5.19 ± 0.30 nm. Between 800 and 1000 microbeads were implanted in each omentum pouch of rats that exhibited characteristics consistent with diabetes after STZ administration. While this treatment was able to normalize glucose levels in many of the animals,[20] a subset of animals did not exhibit improved glucose and were sacrificed upon reaching endpoint criteria based on their poor health resulting from diabetes. The biomaterial grafts in these animals failed to reverse the diabetes. The times ranged from 29 to 37 days (mean = 33 ± 5.7 days). The omenta from these animals were harvested and analyzed by XPC microCT and histology as described below to investigate the reasons for failure in these animals.

XPC μCT

XPC μCT was used to visualize the 3D structure of the tissue and alginate microbeads prior to histological processing. Since biomaterials and soft tissue are hard to visualize with traditional absorption-based X-ray imaging, XPC overcomes these issues via reliance on alternative contrast mechanism such as X-ray refraction.[27] XPC μCT allowed for a nondestructive, three-dimensional analysis of the samples without the need for exogenous contrast agents. The shape and structure of alginate microbeads was observed as well as local soft tissue structure (Fig. 1). To further evaluate the microbeads, the XPC images were registered with H&E stains of the same tissues. Bead structure, omental adipose, and soft tissue formed in response to the beads could all be clearly identified in the XPC and histology images (Fig. 1). This combined approach allowed the identification of failed and stable beads in the samples. Alginate microbeads were classified as failed if they had clear evidence of invading tissue and as stable if the microbeads did not present any tissue invasion [Fig. 1(B)]. The failure rate of alginate microbeads in the omentum pouch was 20.9 ± 0.9% for the beads treated containing islets and 27. 56 ± 16.5% for without islets (p = 0.77).

Histomorphometric analysis

The tissue response around stable and failed beads was then further examined in H&E stained sections. When evaluating the local tissue response, the thickness of the inflammatory layer surrounding the microbeads and the cell density was quantified. The cell density around empty microbeads that failed was $5.6 \pm 1.7 \times 10^3$ cells/mm^2 while the density around stable microbeads was $4.7 \pm 1.5 \times 10^3$ cells/mm^2 (p= 0.229). The thickness

of inflammatory tissues around empty microbeads that failed was of 84.75 ± 49.89 μm while stable microbeads had a thickness of 65.73 ± 17.38 μm (Fig. 2).

When analyzing microbeads containing islets, failed microbeads presented a thicker region of inflammatory tissue surrounding the microbeads (78.86 ± 36.84 μm) than stable microbeads (65.95 ± 29.00 μm, $p = 0.48$) (Fig. 2). The tissue infiltrating the failed microbeads appeared to have a high cellular density [Figs. 2 and 3(A,B)]. Quantitative results supported this observation with a greater density of cells in the tissue invading the failed microbeads ($4.6 \pm 1.4 \times 10^3$ cells/mm^2) when compared to the tissue around stable microbeads [$3.4 \pm 1.9 \times 10^3$ cells/mm^2, $p < 0.05$, Fig. 3(E,F)]. Masson's Trichrome stains were performed for further insight into tissue structure. For beads with islets, collagen (blue) was neither observed in the tissue surrounding the failed [Fig. 3(C,D)] nor stable alginate microbeads with islets [Fig. 3(G,H)] suggesting that the tissue was not going through a constructive remodeling response. Red stained tissues were observed throughout the tissue for beads with and without islets suggesting prolonged inflammation.

Macrophage phenotype

Immunostains for macrophage markers were performed to provide further insight into the tissue response. Immunochemical staining was performed to assess the general presence of macrophages using a pan-macrophage marker ($CD68^+$) and as a first level analysis of the presence of pro-inflammatory ($CCR7^+$) and pro-healing ($CD163^+$) macrophages. Staining of tissue around alginate microbeads with islets indicated the presence of both $CD68^+$ and $CCR7^+$ positive macrophages [Fig. 4(B,C,H,I)]. The presence of $CD68^+$ was observed mostly in regions of the tissue surrounding failed and stable beads as well as in tissue invading failed alginate microbeads. $CCR7^+$ (M1 marker) staining exhibited a similar pattern to $CD68^+$ indicating its presence in failed and stable microbeads. Interestingly, staining was negative for pro-healing macrophages ($CD163^+$) in the samples stained for microbeads with islets [Fig. 4(E,F)]. The spleen control showed that the $CD163^+$ protocol was effective [Fig. 4(D)].

Staining area for $CD68^+$, $CCR7^+$, and $CD163^+$ was quantified for all conditions (Fig. 5). Quantitatively, $CD68^+$ staining was slightly higher around failed microbeads for both conditions. For microbeads with islets, $CCR7^+$ area was higher in failed microbeads (16.0 ± 2.88%) in comparison to stable microbeads with islets (8.67 ± 1.73%, $p = 0.03$). This difference in CCR7 staining was not observed in microbeads without islets. However, $CD163^+$ staining was higher in failed microbeads (9.72 ± 3.38%) without islets in comparison to stable microbeads without islets (5.22 ± 1.59%, $p = 0.2$). When comparing staining data between microbeads with and without islets, stable microbeads with islets had a greater staining for $CD68^+$ cells than without islets (5.26 ± 1.32% vs. 1.52 ± 0.48%, $p = 0.03$).

When examining Masson's Trichrome stains in combination with the immunohistological stains, it is clear that a chronic inflammatory process is occurring throughout the tissue, particularly in the alginate microbeads with islets [Fig. 6(A)]. Collagen formation is present in a portion of alginate microbeads without islets, specifically around stable beads [Fig. 6(B)]. Pro-inflammatory macrophages were observed [Fig. 6(C,D)], and a robust

inflammatory response appears clear in the stains [Fig. 6(A)]. A poor biological response occurred resulting in microbead failure in these animals that did not respond to the encapsulated islets. Pro-healing macrophages were not found around failed or stable beads with islets [Fig. 6(E)], but they were observed around stable and failed microbeads without islets [Fig. 6(F)]. Overall, these data suggest a role for the inflammatory response in microbead failure and possible differences between microbeads loaded with islets and empty microbeads.

DISCUSSION

Alginate-based materials have been investigated for years as a method to encapsulate cells as a treatment for type I diabetes. This approach could potentially overcome limitations related to the shortage in donor islets and the side-effects of chronic immunosuppression. However, the long-term stability of alginate encapsulated islets *in vivo* remains unclear. In many studies, diabetes is “cured” in many animals/patients, while a subset exhibit little or no response to the encapsulated cells.[28] In this study we characterized the stability and tissue response to alginate encapsulated islets in the animals that did not exhibit improved glucose response. The tissues and microbeads were examined by XPC imaging, histological and immunohistochemical method.

The analysis of alginate structure in tissue is challenging as their high water content results in little contrast with many traditional noninvasive imaging modalities and alterations in structure during processing for histology. In our studies, we were able to exploit the novel capabilities of XPC μCT imaging to provide insight into the 3D structure of the beads inside the tissue. While single alginate microbeads can sometimes be identified in tissue sections, histological techniques are limited in their ability to definitively determine the 3D structure of the beads. Tissue processing and sectioning can alter biomaterial structure, making it challenging to unequivocally identify failed beads. XPC allowed improved microbead identification and assessment of 3D tissue invasion, and when combined with histological stains we were able to obtain a more comprehensive view of microbead 3D structure.

Failure rates were similar for microbeads with or without islets. To evaluate the histological response to the microbeads, we first evaluated the encapsulation response. We found that the thickness of inflammatory tissue around the beads was not different for any condition and ranged between 65.73 and 84.75 μm. Thickness of the tissue response can affect solute transport between the host tissue and the encapsulated cells.[29] However, this was not a typical encapsulation response, as cell density was very high and a robust and active inflammatory response was present around both groups of microbeads.

When examining the macrophage response our immunohistochemical staining indicated that the harvested tissue had a high presence of $CD68^{+}$ macrophages. Pro-inflammatory macrophages ($CCR7^{+}$) were higher for failed microbeads with islets and M2 macrophages were not observed in the alginate microbeads with islets indicating the absence of polarization toward the pro-healing phenotype. Macrophage polarization responds to stimuli due to their “cross talk” with other cells and factors around the host response.[30] It is expected that a greater M2 macrophage presence will benefit implantation outcomes.

However, macrophage phenotype is not completely understood. M2 macrophages can be classified as M2a, M2b, M2c. M2a, M2c affect angiogenesis and the overall tissue response while M2b phenotype is believed to have anti-and pro-inflammatory characteristics.[31,32] Different macrophage phenotypes can modulate tissue repair, angiogenesis, and vascularization of implanted biomaterials. Surface material can vary macrophage-surface interactions.[14,33]

In this study, two surface markers (CCR7, CD163) were used to determine macrophage phenotype. Additional studies are required to determine longer effects of macrophage phenotype. Regardless, when our macrophage results are combined with the robust inflammatory response observed in the Masson's Trichrome stains and the high failure rates in microbeads, it suggests that failure was accompanied by a pro-inflammatory environment particularly in the microbeads with islets since staining for pro-healing macrophages was negative. $CD163^{+}$ was observed in failed and stable beads without islets and a small portion of microbeads without islets indicated the presence of collagen suggesting some formation of granulation tissue.

Alginate microbeads can fail due to several reasons. However, in this case only a small subset failed through what appeared to result from a robust inflammatory response. Failure was not due to encapsulation around stable biomaterials which hindered islet performance. Instead, the failure was due to breakdown of the microbeads. The failure indicated in our studies was not only observed around the failed microbeads but was present throughout the omentum. It is not clear why failure occurs in some animals. It may be due to the surgical procedure. However, this would be a very high rate of surgical failure and our samples do not indicate signs of infection. More likely is that a small fraction of the beads fail, and when they do fail it stimulates a prolonged inflammatory process. This increased inflammation results in the failure of other microbeads, which further affects the inflammatory cycle. Possible reasons for alginate microbeads failure are exposure of the PLO layer. Our beads are coated with PLO with an outer alginate layer, which is present to increase stability and reduce the immune response. However, if this layer is eroded, exposure of the PLO can result in a greater host response inducing bead failure.[34] Under physiological conditions the outer layer of alginate could be exposed due to enzymatic and hydrolytic degradation leading to overgrowth and immune rejection.[35]

Other reasons for alginate failure could be the pH of the implantation site and the molecular weight of alginate influencing degradation.[5] The alginate conditions used were 1.5% high mannuronic acid for the inner layer and 1.25% high-guluronic acid. Studies have shown that different concentrations of mannuronic acid or guluronic acid and alginate purity affect the immune response and capsule overgrowth.[29,36] The conditions chosen for islet encapsulation have been previously shown to allow encapsulation of islets that maintain function *in vitro* and *in vivo*. Previous studies have shown that alginate with 1.5% high mannuronic acid successfully encapsulate islets that can have a prolonged response *in vivo*.[18,20,26] The 1.25% high-guluronic acid conditions used to form the multilayer alginate structures enables prolonged release of proteins from the encapsulated cells. [18]

In conclusion, alginate microbeads in animals who were unable to achieve sustained glucose control were characterized by XPC microCT, histology, and immunostaining. Failure rates, histomorphometric analyses and immunostaining allowed the quantification and identification of failure characteristics of alginate microbeads. A robust inflammatory response was observed throughout the tissue suggesting that failure occurred due to a poor tissue response following implantation. Future research should be performed to provide insight into why failure occurred in only a subset of animals. Understanding long-term biomaterial stability and tissue response can inform the design of new therapeutic approaches.

Acknowledgments

Contract grant sponsor: National Science Foundation; contract grant numbers: CBET-1263994, EEC-1157041, EEC-1461215

Contract grant sponsor: Veterans Administration; contract grant number: 5 I01 BX000418-06

Contract grant sponsor: Armour College of Engineering R&D program

References

1. Opara EC, Mirmalek-Sani S-H, Khanna O, Moya ML, Brey EM. Design of a bioartificial pancreas. J Invest Med. 2011; 58:831–837.
2. Pareta RA, Farney AC, Opara EC. Design of a bioartificial pancreas. Pathobiology. 2013; 80:194–202. [PubMed: 23652283]
3. Robitaille R, Dusseault J, Henley N, Desbiens K, Labrecque N, Halle JP. Inflammatory response to peritoneal implantation of alginate–poly-l-lysine microcapsules. Biomaterials. 2005; 26:4119–4127. [PubMed: 15664639]
4. Kollmer M, Appel AA, Somo SI, Brey E. Long-term function of alginate encapsulated islets. Tissue Eng Part B Rev Forthcoming. 2016; 22:34–46.
5. Sun J, Tan H. Alginate-based biomaterials for regenerative medicine applications. Materials (Basel). 2013; 6:1285–1309. [PubMed: 28809210]
6. Moya ML, Morley M, Khanna O, Opara EC, Brey E. Stability of alginate microbead properties in vitro. J Mater Sci Mater Med. 2012; 23:903–912. [PubMed: 22350778]
7. Capone SH, Dufresne M, Rechel M, Fleury MJ, Salsac AV, Paullier P, Daujat-Chavanieu M, Legallais C. Impact of alginate composition: From bead mechanical properties to encapsulated HepG2/C3A cell activities for in vivo implantation. PLoS One. 2013; 8:e62032. [PubMed: 23637958]
8. Ponce S, Orive G, Hernandez R, Gascon AR, Pedras JL, de Haan BJ, Faas MM, Mathieu HJ, de Vos P. Chemistry and the biological response against immunoisolating alginate–polycation capsules of different composition. Biomaterials. 2006; 27:4831–4839. [PubMed: 16766026]
9. Zhu H, Lu L, Liu X, Yu L, Lyu Y, Wang B. Treatment of diabetes with encapsulated pig islets: An update on current developments. J Zhejiang Univ Sci B. 2015; 16:329–343. [PubMed: 25990050]
10. Zakrzewski JL, van den Brink MR, Hubbell JA. Overcoming immunological barriers in regenerative medicine. Nat Biotechnol. 2014; 32:786–794. [PubMed: 25093888]
11. Dufrane D, Goebbels RM, Saliez A, Guiot Y, Gianello P. Six-month survival of microencapsulated pig islets and alginate biocompatibility in primates: Proof of concept. Transplantation. 2006; 81:1345–1353. [PubMed: 16699465]
12. Anderson JM, McNally A. Biocompatibility of implants: Lymphocyte/macrophage interactions. Semin Immunopathol. 2011; 33:221–233. [PubMed: 21271251]
13. Garg K, Pullen NA, Oskeritzian CA, Ryan JJ, Bowlin G. Macrophage functional polarization (M1/M2) in response to varying fiber and pore dimensions of electrospun scaffolds. Biomaterials. 2013; 34:4439–4451. [PubMed: 23515178]

14. Badylak SF, Valentin JE, Ravindra AK, McCabe GP, Stewart-Akers A. Macrophage phenotype as a determinant of biologic scaffold remodeling. Tissue Eng A. 2008; 14:1835–1842.
15. Umashankar PR, Arun T, Kumary T. Effect of chronic inflammation and immune response on regeneration induced by decellularized bovine pericardium. J Biomed Mater Res A. 2013; 101A: 2202–2209.
16. Lacy PE, Kostianovsky M. Method for the isolation of intact islets of langerhans from the rat pancreas. Diabetes. 1967; 16:35–39. [PubMed: 5333500]
17. Field J, Farney A, Sutherland D. Improved islet isolation from rat pancreas using 35% bovine serum albumin in combination with Dextran gradient separation. Transplantation. 1996; 61:1554–1556. [PubMed: 8633389]
18. Khanna O, Moya ML, Opara EC, Brey E. Synthesis of multilayered alginate microcapsules for the sustained release of fibroblast growth factor-1. J Biomed Mater Res A. 2010; 95:632–640. [PubMed: 20725969]
19. Darrabie MD, Kendall WF, Opara E. Characteristics of poly-l-ornithine-coated alginate microcapsules. Biomaterials. 2005; 26:6846–6852. [PubMed: 15955558]
20. Pareta R, McQuilling JP, Sittadjody S, Jenkins R, Bowden S, Orlando G, Farney AC, Brey EM, Opara EC. Long-term function of islets encapsulated in a redesigned alginate microcapsule construct in omentum pouches of immune-competent diabetic rats. Pancreas. 2014; 43:605–613. [PubMed: 24681880]
21. Zhong Z, Thomlinson W, Chapman D, Sayers D. Implementation of diffraction-enhanced imaging experiments: At the NSLS and APS. Nucl Inst Methods Phys Res Sect A Accel Spectrometers Detect Assoc Equip. 2000; 450:556–567.
22. Appel AA, Larson JC, Somo S, Zhon Z, Spicer PP, Kasper FK, Garson AB III, Zysk AM, Mikos AG, Anastasio MA, Brey EM. Imaging of poly(α-hydroxy-ester) scaffolds with x-ray phase-contrast microcomputed tomography. Tissue Eng Part C Methods. 2012; 18:859–865. [PubMed: 22607529]
23. Brankov JG, Wernick MN, Li J, Muehleman C, Zhong Z, Anastasio MA. A computed tomography implementation of multiple-image radiography. Med Phys. 2006; 33:278–289. [PubMed: 16532932]
24. Chou CY, Anastasio MA, Brankov JG, Wernick MN, Brey EM, Connor DM Jr, Zhong Z. An extended diffraction-enhanced imaging method for implementing multiple-image radiography. Phys Med Biol. 2007; 52:1923–1945. [PubMed: 17374920]
25. Wernick MN, Wirjadi O, Chapman DZhong Z, Galatsanos NP, Yang Y, Brankov JG, Oltulu O, Anastasio MA, Muehleman C. Multiple-image radiography. Phys Med Biol. 2003; 48:3875–3895. [PubMed: 14703164]
26. McQuilling JP, Arenas-Herrera J, Childers C, Pareta RA, Khanna O, Jiang B, Brey EM, Farney AC, Opara EC. New alginate micro-capsule system for angiogenic protein delivery and immunoisolation of islets for transplantation in the rat omentum pouch. Transplant Proc. 2011; 43:3262–3264. [PubMed: 22099771]
27. Appel AA, Larson JC, Garson AB III, Guan H, Zhong Z, Nguyen BN, Fisher JP, Anastasio MA, Brey EM. X-ray phase contrast imaging of calcified tissue and biomaterial structure in bioreactor engineered tissues. Biotechnol Bioeng. 2015; 112:612–620. [PubMed: 25257802]
28. Sun Y, Ma X, Zhou D, Vacek I, Sun A. Normalization of diabetes in spontaneously diabetic cynomologus monkeys by xenografts of microencapsulated porcine islets without immunosuppression. J Clin Invest. 1996; 98:1417–1422. [PubMed: 8823307]
29. King A, Sandler S, Andersson A. The effect of host factors and capsule composition on the cellular overgrowth on implanted alginate capsules. J Biomed Mater Res. 2001; 57:374–383. [PubMed: 11523032]
30. Brown BN, Valentin JE, Stewart-Akers AM, McCabe GP, Badylak S. Macrophage phenotype and remodeling outcomes in response to biologic scaffolds with and without a cellular component. Bio-materials. 2009; 30:1482–1491.
31. Spiller KL, Anfang RR, Spiller KJ, Ng J, Nakazawa KR, Daulton JW, Vunjak-Novakovic G. The role of macrophage phenotype in vascularization of tissue engineering scaffolds. Biomaterials. 2014; 35:4477–4488. [PubMed: 24589361]

32. Mokarram N, Merchant A, Mukhatyar V, Patel G, Bellamkonda R. Effect of modulating macrophage phenotype on peripheral nerve repair. Biomaterials. 2012; 33:8793–8801. [PubMed: 22979988]

33. Bartneck M, Heffels KH, Pan Y, Bovi M, Zwadlo-Klarwaser G, Groll J. Biomaterials Inducing healing-like human primary macrophage phenotypes by 3D hydrogel coated nano fibres. Biomaterials. 2012; 33:4136–4146. [PubMed: 22417617]

34. Tam SK, Bilodeau S, Dusseault J, Langlois J, Halle JP, Yahia LH. Biocompatibility and physicochemical characteristics of alginate–polycation microcapsules. Acta Biomater. 2011; 7:1683–1692. [PubMed: 21145438]

35. Hillberg AL, Kathirgamanathan K, Lam JB, Law LY, Garkavenko O, Elliot RB. Improving alginate-poly-ornithine-alginate capsule biocompatibility through genipin crosslinking. J Biomed Mater Res Part B Appl Biomater. 2013; 101B:258–268.

36. Uludag H, De Vos P, Tresco P. Technology of mammalian cell encapsulation. Adv Drug Deliv Rev. 2000; 42:29–64. [PubMed: 10942814]

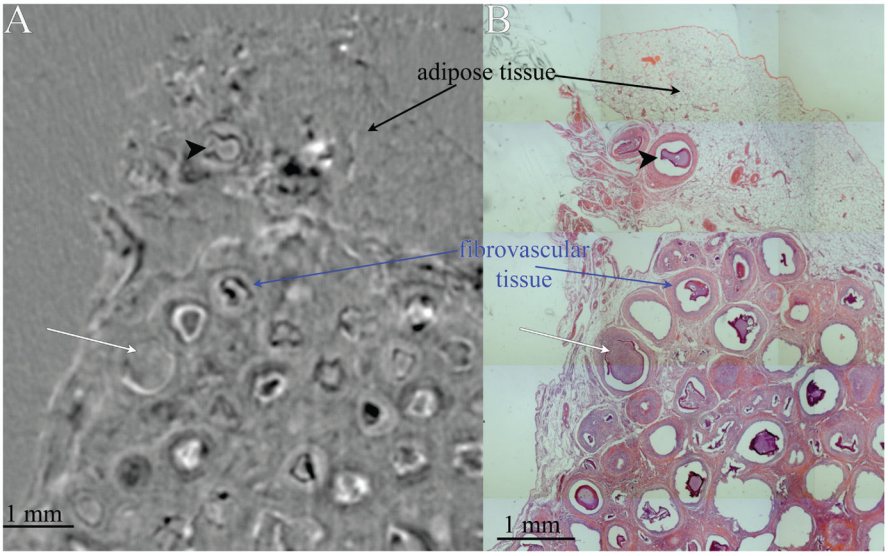

FIGURE 1.

(A) Slice from XPC Refraction μCT and (B) corresponding H&E section. Adipose tissue can be distinguished from fibrovascular tissue that formed in response to the beads. Alginate beads can also be identified, failed microbeads (white arrow) and stable microbeads (black arrowhead).

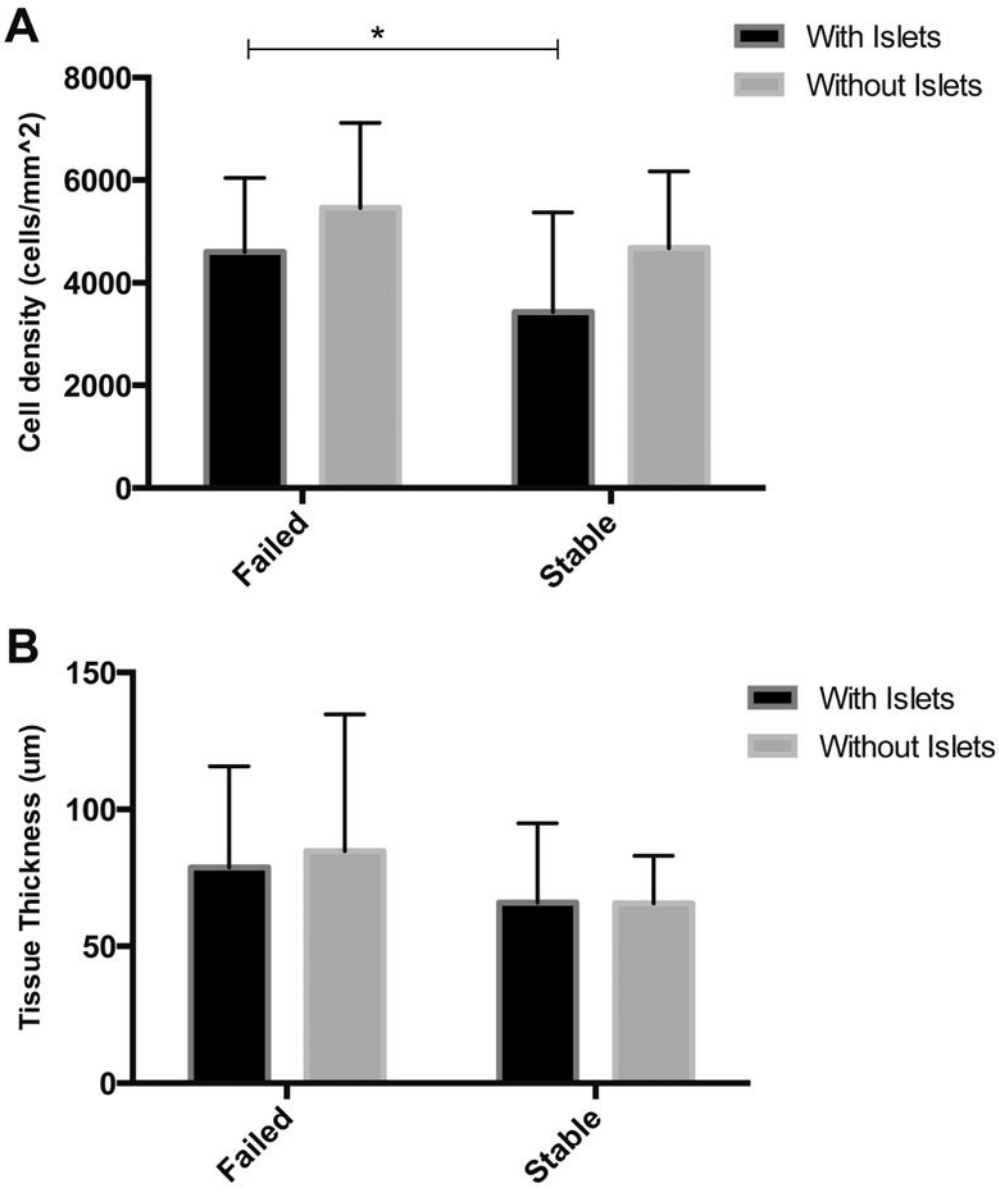

FIGURE 2.

(A) Failed microbeads have a higher number of cells in the tissue surrounding alginate microbeads. (B) Failed microbeads have a thicker layer of tissue around the bead $p = 0.48$. * indicates $p < 0.05$.

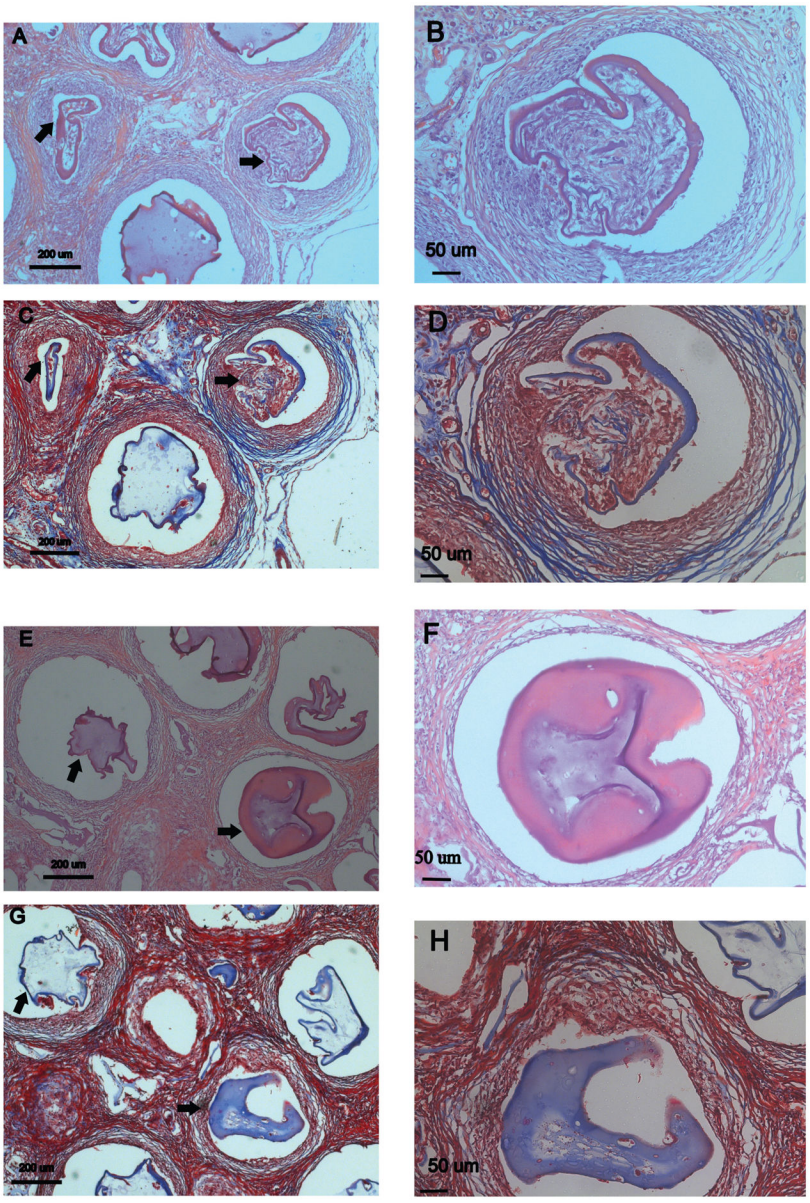

FIGURE 3.

H&E and Masson's Trichrome images of stable and failed alginate microbeads. Failed beads (A–D) exhibit characteristics of a chronic inflammatory response indicated by a high cell density (B). The thickness of the inflammatory tissue surrounding failed alginate microbeads was greater than stable microbeads. Stable beads (E–H) show a lower number of cells surrounding the alginate microbeads (F). Masson's Trichrome indicates a high inflammation response in both failed and stable beads (C, D, G, H). Arrows indicate failed and stable beads.

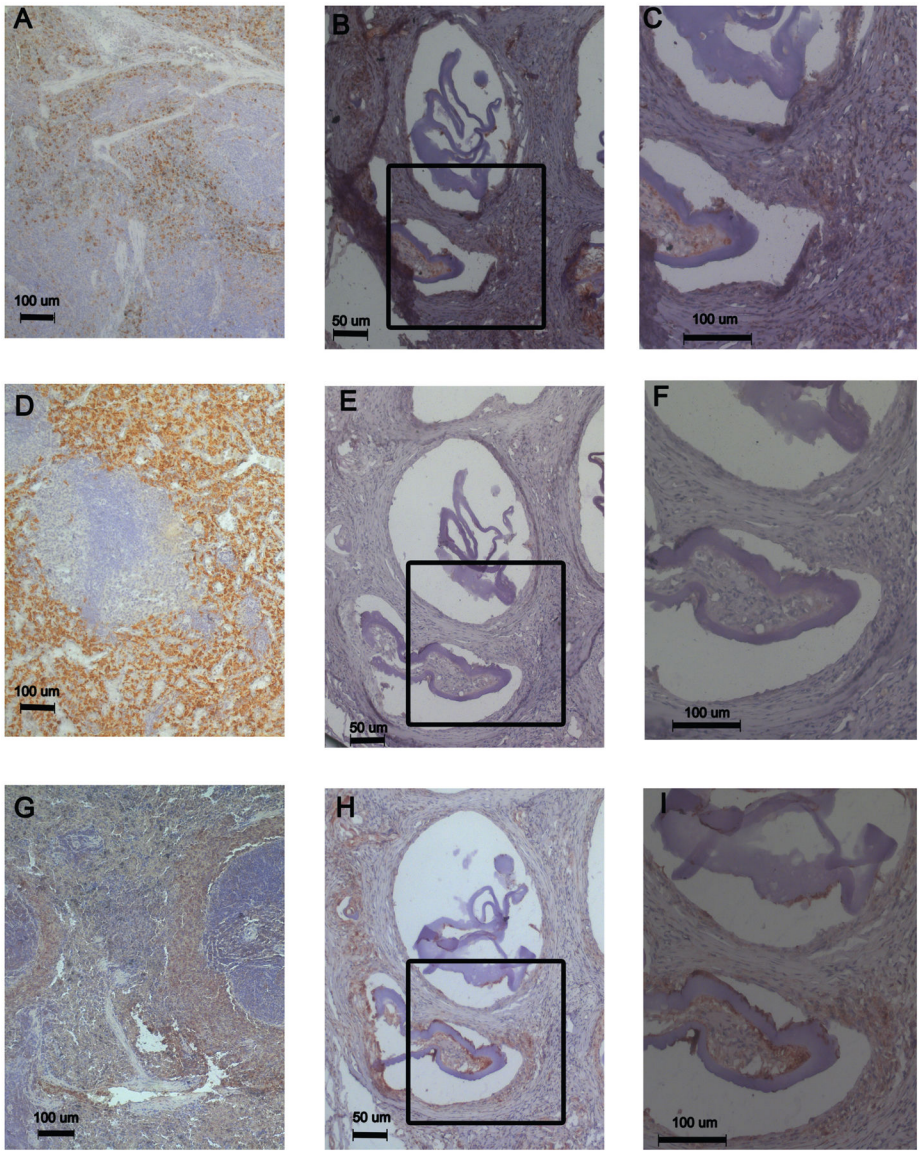

FIGURE 4.

Immunohistochemical staining around alginate microbeads. Spleen was used as a control for markers CD68 (A), CD163 (D), CCR7 (G). $CD68^+$ stain is observed (B, C)as well as $CCR7^+$ (H,I). $CD163^+$ staining was not observed (E, F). (C, F, I) higher resolution images of the inset area.

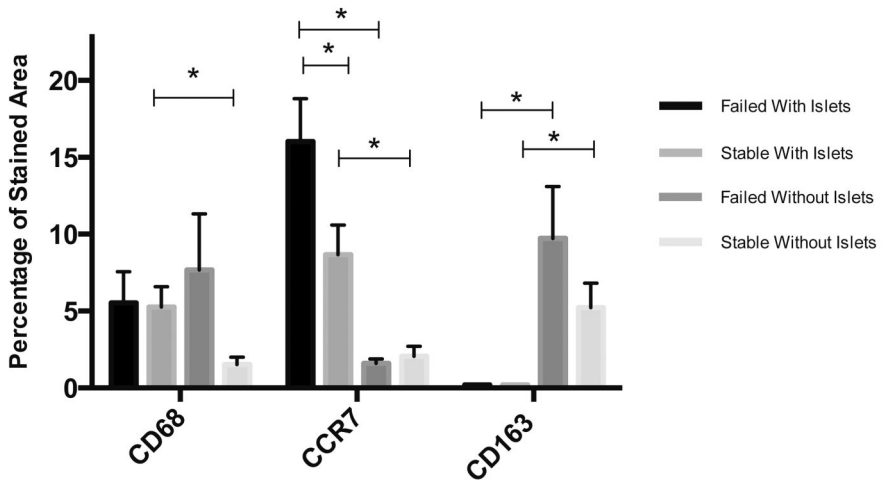

FIGURE 5.

Quantitative analysis of staining for macrophage markers. * indicates p values < 0.05. Error bars indicate standard error.

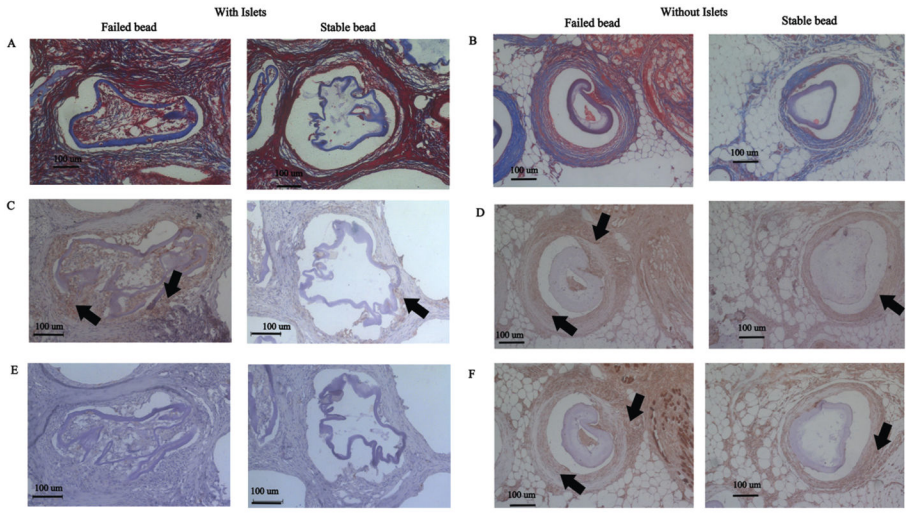

FIGURE 6.

Masson's Trichrome (A, B) indicates the presence of a chronic inflammatory response (red color) around both stable and failed alginate microbeads with islets and the presence of collagen for a small subset of alginate microbeads without islets. CCR7 stain indicates the presence of inflammatory macrophages (M1) in stable and failed alginate microbeads (C,D) while CD163 pro-healing macrophage phenotype (M2) was not observed in the groups with islets (E), the presence of pro-healing macrophage ($CD163^{+}$) is observed in stable and failed alginate microbeads without islets (F). Arrows indicate macrophage presence.